Available online at www.sciencedirect.com
ScienceDirect
Biochimie 91 (2009) 204–213
BIOCHIMIE
www.elsevier.com/locate/biochi

Research paper

UDPglucose pyrophosphorylase from *Xanthomonas* spp. Characterization of the enzyme kinetics, structure and inactivation related to oligomeric dissociation

M.B. Bosco, M. Machtey, A.A. Iglesias, M. Aleanzi*

Laboratorio de Enzimología Molecular, Facultad de Bioquímica y Ciencias Biológicas, Universidad Nacional del Litoral, Paraje ''El Pozo'', CC 242, Santa Fe (S3000ZAA), Argentina

Received 4 June 2008; accepted 3 September 2008
Available online 25 September 2008

Abstract

The genes encoding for UDPglucose pyrophosphorylase in two *Xanthomonas* spp. were cloned and overexpressed in *Escherichia coli*. After purification to electrophoretic homogeneity, the recombinant proteins were characterized, and both exhibited similar structural and kinetic properties. They were identified as dimeric proteins of molecular mass 60 kDa, exhibiting relatively high specific activity (~80 Units/mg) for UDPglucose synthesis. Both enzymes utilized UTP or TTP as substrate with similar affinity. The purified *Xanthomonas* enzyme was inactivated after dilution into the assay medium. Studies of crosslinking with the bifunctional lysyl reagent bisuberate suggest that inactivation occurs by enzyme dissociation to monomers. UTP effectively protects the enzyme against inactivation, from which a dissociation constant of 15 μM was calculated for the interaction substrate-enzyme. The UTP binding to the enzyme would induce conformational changes in the protein, favoring the subunits interaction to form an active dimer. This view was reinforced by protein modeling of the *Xanthomonas* enzyme on the basis of the prokaryotic UDPglucose pyrophosphorylase crystallographic structure. The in silico approach pointed out two main critical regions in the enzyme involved in subunit-subunit interaction: the region surrounding the catalytic-substrate binding site and the C-term.

Keywords: UDPglucose pyrophosphorylase; Polysaccharides; *Xanthomonas*; Oligomeric dissociation

1. Introduction

UDPGlc pyrophosphorylase (EC 2.7.7.9; UDPGlcPPase) catalyzes the reversible production of UDPGlc and PPi from UTP and glucose-1-phosphate (Glc1P) in the presence of a divalent metal cation (mainly Mg^{2+}) [1]. The sugar-nucleotide thus synthesized plays a pivotal role in carbohydrate metabolism in different organisms. UDPGlc is the substrate for UDP-glucuronic acid synthesis, and it is necessary for galactose and glucose interconversion through the Leloir pathway [2]. Also, the sugar-nucleotide is a precursor metabolite in the routes conducting to different oligo- and polysaccharides [3–5]. UDPGlcPPase is ubiquitous in nature, being found in animals, plants and microorganisms. Outstandingly, the eukaryotic and prokaryotic forms of the enzyme are completely unrelated, with main differences at the level of amino acids sequence and three-dimensional structure [4,6,7].

Since UDPGlcPPase is involved in producing glycosyl donors for lipopolysaccharide and capsule biosynthesis, the enzyme is critical for virulence in *Streptococcus pneumoniae* [8] and many other bacteria, including Gram-positive and Gram-negative species [9–12]. Also the synthesis of bacterial exopolysaccharides is strictly linked to UDPGlc. Examples are the production of gellan by *Sphingomonas elodea* [13] and of xanthan gum by *Xanthomonas* sp. [14,15]. The latter polymer is utilized in a wide range of industrial processes [14]. *Xanthomonas campestris* and *Xanthomonas axonopodis* are,

* Corresponding author. Tel. +54 342 457 5216x217; fax: +54 342 457 5216.
E-mail address: maleanzi@fbcb.unl.edu.ar (M. Aleanzi).

0300-9084/$ - see front matter © 2008 Elsevier Masson SAS. All rights reserved.
doi:10.1016/j.biochi.2008.09.001

respectively, the causative agents of black rot in cruciferous plants [16] and canker in citrus [15,17]. In the development of plant infection, xanthan gum produced by these bacteria is critical for improving the efficiency of colonization [15]. The gene coding for UDPGlcPPase in *X. campestris* has been cloned and expressed to restore the mucoid phenotype of the G76E *Xanthomonas* mutant [18].

Despite the relevance of xanthan gum in commercial issues, related with *Xanthomonas* sp. virulence towards fruit plants and with industrial uses of the polymer, reports on the study of the enzymes involved in the biosynthesis of the exopolysaccharide are scarce. In the present work we perform the molecular cloning of the genes encoding for UDPGlcPPase in *X. campestris* and *X. axonopodis*. The respective recombinant enzymes were purified and characterized kinetically. It is shown that the enzyme from *Xanthomonas* sp. distinctively exhibits high specific activity and it undergoes inactivation associated with subunits dissociation that is prevented by the substrate UTP.

2. Materials and methods

2.1. Materials

Bacteriological media components were from Britania Laboratories (Rosario, Santa Fe, Argentina). Enzymes for molecular biology protocols were from Promega. UTP, TTP, UDPGlc and Glc1P were from Sigma (St. Louis, MO, USA). All other chemicals were of the highest quality commercially available.

2.2. Bacterial strains and plasmids

Dr. Luis Ielpi (Fundación Instituto Leloir, Buenos Aires, Argentina) and Dr. Adrián A. Vojnov (Fundación Pablo Cassará, Buenos Aires, Argentina) kindly provided strains of *X. campestris* pv. campestris and *X. axonopodis* pv. citri, respectively. *Xanthomonas* strains were grown in YM media [19]. *Escherichia coli* Top 10 (Invitrogen) cells and *E. coli* BL21(DE3) were utilized in routine plasmid construction and expression experiments, respectively. The vector pGEM-T Easy (Promega) was utilized for cloning and sequencing purposes. The expression vector was pET-24a (Novagen). DNA manipulation, *E. coli* culture and transformation were performed according to standard protocols [20].

2.3. Molecular cloning and construction of the expression vectors

The genes were amplified from genomic DNA of the respective *Xanthomonas* sp., by utilizing PCR techniques. Oligonucleotide primer pairs utilized for PCR amplification were designed from sequences available in the NCBI database, as described in Table 1. The protocol for PCR was: 94 °C for 10 min; 30 cycles of 94 °C for 1 min, 55 °C for 1 min, and 72 °C for 1 min; then 72 °C for 10 min. The PCR product was purified and ligated into the pGEM-T Easy vector to ease further work. The fidelity and correctness of each gene were confirmed on both strands by complete DNA sequencing.

Table 1
Oligonucleotide primer pairs utilized for PCR amplification designed from sequences available in the NCBI database

Primers	*X. campestris*	*X. axonopodis*
Forward	*Nde*I, 5′-AAG ACT CAT ATG AGC AAG CGT ATT CGC-3′	*Nde*I, 5′-CAT ATG AGC CAG CGT ATT CGC AAG-3′
Reverse	*Sac*I, 5′-ATG GCA GAG CTC TCA AGC ATG GCA CCA-3′	*Bam*HI, 5′-GGA TCC TCA GCC GCG CAC GTC-3′

The cloned plasmids and the pET-24a vector were digested with the respective pair of restriction enzymes: *Nde*I/*Sac*I (*X. campestris*) and *Nde*I/*Bam*HI (*X. axonopodis*). Restriction fragments were purified by gel extraction after gel electrophoresis. Ligation to the pET-24a vector of each insert was performed using T4 DNA ligase for 16 h at 10 °C. Competent *E. coli* BL21(DE3) cells were transformed with the respective expression plasmid. Transformed cells were selected in agar plates containing Luria-Bertani broth (LB; 10 g/l NaCl, 5 g/l yeast extract, 10 g/l peptone, pH 7.4) supplemented with 50 μg/ml kanamycin. The correctness of the expression constructs was checked by preparation of plasmid DNA followed by analysis of treatments with the respective restriction enzymes.

2.4. Overexpression and purification of recombinant UDPGlcPPase

Identical conditions were followed to express and purify recombinant UDPGlcPPase from *X. campestris* or *X. axonopodis*. Single colonies of *E. coli* BL21(DE3) transformed with the respective recombinant plasmid were selected. Overnight cultures were 1/100 diluted in fresh LB medium, supplemented with 50 μg/ml kanamycin, and grown at 37 °C up to $OD_{600} = 0.6$. The expression was induced at 28 °C, for 13 h with 0.2 mM IPTG, after which cells were chilled on ice and harvested by centrifugation. All subsequent purification steps were conducted at 0–4 °C. The cell paste was resuspended in buffer A (50 mM Mops-NaOH, pH 8.0, 5 mM $MgCl_2$, 0.1 mM EDTA, 5 mM DTT, and 5% w/v sucrose), disrupted by sonication and the lysates were clarified by centrifugation. The resulted crude extract was fractionated with a 30–80% ammonium sulfate cut. After centrifugation, the pellet was redissolved in buffer A and desalted on Bio-Rad 10 DG chromatography columns equilibrated with the same buffer. The desalted sample was applied to a DEAE-Sepharose column, equilibrated with buffer A, and eluted with a linear NaCl gradient (0–0.5 M). The purest fractions (as visualized by PAGE) were pooled, conveniently concentrated with Centricon-10 devices (Amicon Inc.) and, after addition of glycerol (to 20% v/v final concentration) stored at −80 °C. Under these conditions the enzyme remained stable for at least 3 months.

2.5. Enzymatic activity and protein assays

UDPGlcPPase activity, either in the UDPGlc synthesis or pyrophosphorolysis directions was followed by procedures

previously developed for measurement of ADPglucose pyrophosphorylase [21,22]. Enzyme activity in the UDPGlc synthesis direction was assayed by following the formation of Pi (after hydrolysis of PPi by inorganic pyrophosphatase) by the colorimetric method described by Fusari et al. [21]. The assays were performed at 37 °C in a reaction mixture containing (unless otherwise specified) 100 mM Mops-NaOH (pH 8.0), 7 mM $MgCl_2$, 1.5 mM UTP, 1 mM Glc1P, 0.2 mg/ml BSA, 1.5 U/ml inorganic pyrophosphatase, plus enzyme in a final volume of 50 µl. The reaction was stopped with the addition of 50 µl of color reagent (see Ref. [21] for details) and read at 650 nm with a Spectramax (Molecular Devices) 96-well microplate reader.

In the UDPGlc pyrophosphorolysis direction, formation [^{32}P]UTP from [^{32}P]PPi was determined after [22]. The standard aqueous reaction mixture contained 80 mM Mops-NaOH (pH 8.0), 5 mM $MgCl_2$, 1.5 mM [^{32}P]PPi (500–2500 cpm/nmol), 1.5 mM UDPGlc, 4 mM NaF, 0.2 mg/ml BSA, plus enzyme in a total volume of 250 µl. After 10 min of incubation at 37 °C, the reaction was terminated by the addition of 3 ml of cold 5% w/v trichloroacetic acid. The [^{32}P]UTP formed was bound to activated carbon (15% w/v Norite A in 100 mM PPi). After washing twice the UTP-bound carbon with 5% w/v trichloroacetic acid, [^{32}P]UTP was hydrolyzed by the addition of 1 M HCl and boiling for 10 min. The released radioactivity was measured in a scintillation counter.

Under the conditions above described for enzyme assay of synthesis or pyrophosphorolysis directions, one unit (U) of enzyme activity is defined by the production of 1 µmol of product, either PPi (which renders 2 µmol of Pi after hydrolysis) or [^{32}P]UTP, formed per minute.

Protein contents were determined by the method of Bradford [23], using BSA as a standard.

2.6. Kinetic characterization

The kinetic data were plotted as initial activity (expressed as specific activity; U/mg) versus substrate concentration ([S]). Data were fitted to the Hill equation with the Levenberg–Marquardt nonlinear least-squares algorithm provided by the computer program Origin 7.0, to calculate kinetic constants: V_{max}, the enzyme maximal velocity; $S_{0.5}$, the concentration of substrate giving 50% of V_{max}; and n_H, the Hill coefficient. Kinetic constants are the mean of at least three independent sets of data, and they are reproducible within ±10%.

2.7. Protein electrophoresis

Polyacrylamide gel electrophoresis (PAGE) under native and denatured (SDS-PAGE) conditions were performed as described by Laemmli [24], using the Bio-Rad minigel apparatus. Coomasie brilliant blue was utilized to stain protein bands. For molecular mass estimation of native enzyme, PAGE was conducted on gels of increasing monomer concentration (6.5–10.5% w/v total acrylamide concentration). Gels were calibrated by running proteins of known molecular mass and plotting log of the relative migration versus gel concentration, according to Ferguson [25]. SDS-PAGE was developed on discontinuous gels, with final monomer concentrations of 4% and 15% w/v acrylamide, for the stacking and separating gels, respectively.

Analysis of oligomeric structures stabilized by crosslinking was carried by the procedure developed by Staros [26]. Samples of purified UDPGlcPPase were incubated at 37 °C during 30 min in a medium containing Mops-NaOH (pH 8.0), 1 mg/ml of enzyme, and 0.1 mM bisuberate in a final volume of 110 µl. When specified, different substrates were included in the incubation medium. The reaction of modification with bisuberate was stopped by the addition of 15 µl of 50 mM ethanolamine in buffer Mops, and the samples were then analyzed by SDS-PAGE.

2.8. Structure prediction analysis

The homology model for the dimer of Xanthomonas spp. UDPGlcPPase was built using the program Modeller 9v2 [27–31]. Both known crystallographic structures of prokaryotic UDPGlcPPases, the tight dimer (chains AC) protein from *E. coli* (deposited in the Protein Data Bank as 2E3D), and the tight dimer (chains BC) enzyme from *Corynebacterium glutamicum* complexed with 2 mol of Mg^{2+} per mol of enzyme subunit (deposited in the Protein Data Bank as 2PA4), were used as templates. Sequence alignment performed with BioEdit 7.0.9.0 software (http://www.mbio.ncsu.edu/BioEdit/BioEdit.html) was modified manually considering the secondary structure of the templates. Gaps were avoided in secondary structure elements and in buried regions [30]. The model was checked with three-dimensional profiles using the program Verfy3D (http://nihserver.mbi.ucla.edu/Verify_3D/) and the alignment was corrected iteratively according to the profiles. Model illustrations were made with VMD software (http://www.ks.uiuc.edu/).

3. Results and discussion

The sequence of the gene *galU*, coding for UDPGlcPPase, is available in the genome databases of *X. campestris* pv. campestris (*Xca*) [http://www.ncbi.nlm.nih.gov; XC_1930, gene ID 3389471] and *X. axonopodis* pv. citri (*Xax*) [http://www.ncbi.nlm.nih.gov; XAC2292, gene ID 1156363]. Each gene respectively codes for proteins of 297 (*Xca*UDPGlcPPase) and 294 (*Xax*UDPGlcPPase) amino acids; and these UDPGlcPPases share 95% identity. We cloned *galU* from the two *Xanthomonas* spp by PCR amplification, utilizing genomic DNA and specifically designed oligonucleotide primers. The correctness of each cloned gene was confirmed by complete sequence. As shown in Fig. 1, *Xca*UDPGlcPPase was overexpressed in *E. coli* cells and purified to over 90% homogeneity after ammonium sulfate fractionation and ion-exchange chromatography. Essentially identical results were obtained for the expression and purification of the enzyme from *Xax* (data not shown). Both recombinant enzymes exhibited a dimeric structure when analyzed by native PAGE performed at different acrylamide concentrations (Fig. 2).

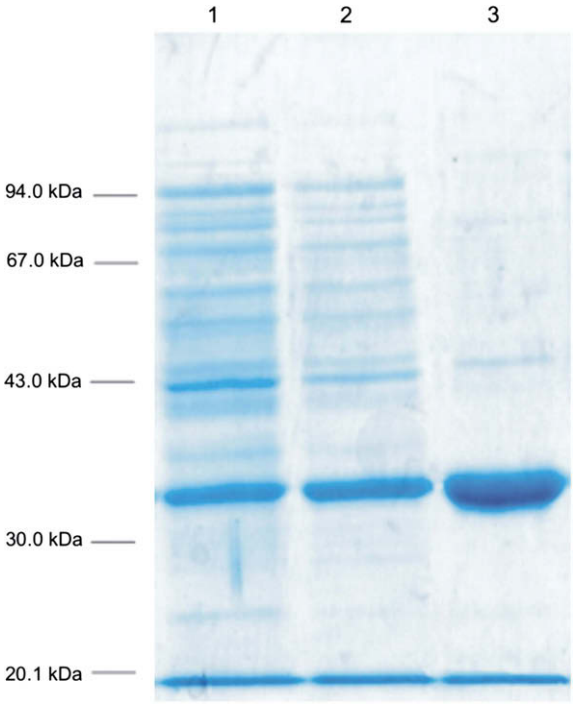

Fig. 1. SDS-PAGE analysis of the purification of recombinant *Xca*UDPGlcPPase. Lanes: 1, crude extract; 2, ammonium sulfate (30–80% saturation) fractionation; 3, enzyme recovered after ion-exchange chromatography. Each lane contained 8 μg of total protein. Molecular mass markers: phosphorylase b (97 kDa), BSA (66 kDa), ovoalbumin (45 kDa), carbonic anhydrase (30 kDa), trypsin inhibitor (20.1 kDa).

Thus, each enzyme migrated as a single protein band in native PAGE (Fig. 2A), and the respective retardation in migration was proportional to the increased degree of acrylamide polymerization in the gel when the data were fitted according to Ferguson plots (Fig. 2B) [25]. As shown in the inset of Fig. 2B, the plots of the log of relative mobility versus gel concentration were linear for both recombinant enzymes, although they gave parallel lines, as expected for globular proteins with different isoelectric points [32,33]. In good agreement with the latter, different theoretical pI values of 5.45 and 5.64 were calculated for UDPGlcPPase from *Xca* and *Xax*, respectively; according to on-line ExPASy at http://ca.expasy.org.

The recombinant proteins were active as UDPGlcPPases, and they displayed a higher (about 7-fold) V_{max} for the reaction of UDPGlc synthesis compared to pyrophosphorolysis. Both enzymes exhibited kinetic parameters basically similar to those detailed in Table 2 for *Xca*UDPGlcPPase. The enzymes showed neither activity with ATP, nor with GTP; but they utilized TTP to synthesize TDPGlc. The catalytic efficiency with TTP was one order of magnitude lower than with UTP, because of the higher k_{cat} and lower $S_{0.5}$ exhibited with the latter nucleotide (Table 3). Remarkable is the specific activity in the UDPGlc synthesis direction determined for the *Xanthomonas* enzyme, as the value of 60–90 U/mg is significantly higher than those reported for UDPGlcPPase from *E. coli* (4.8 U/mg) [5], *S. elodea* (1.3 U/mg) [13] and *S. pneumoniae* (13.4 U/mg) [8].

The kinetic parameters showed in Tables 2 and 3 were determined by commencing assays for activity by the addition of purified UDPGlcPPase. When the assays were started with a substrate after preincubation of the enzyme into the assay medium, results were different depending on the nature of the incubated substrate. Fig. 3 shows the saturation kinetics for Glc1P of the enzyme from *Xca*, obtained when the reaction was initiated with the variable substrate or with UTP. As

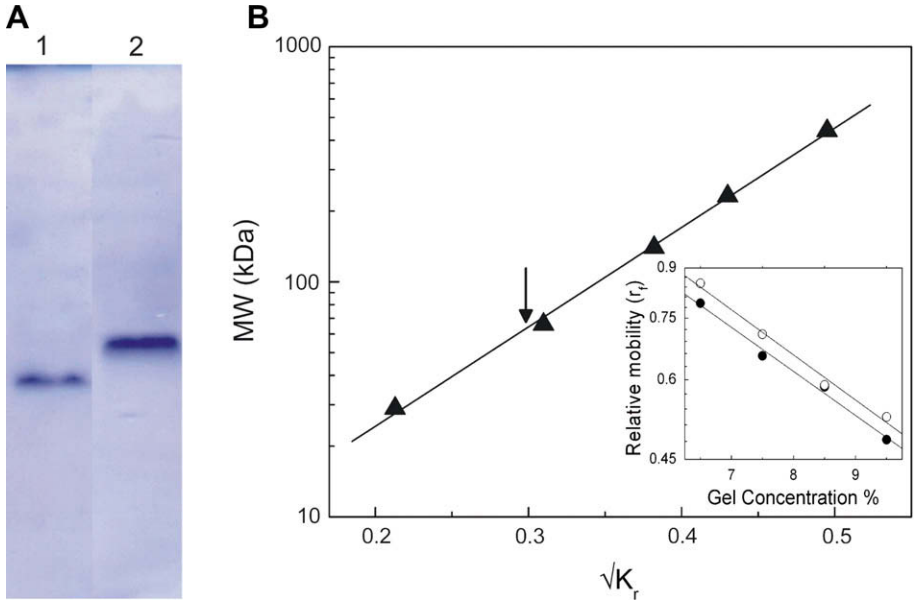

Fig. 2. Native PAGE of purified *Xca*- and *Xax*UDPGlcPPases. (A) PAGE at 8.5% (w/v) acrylamide gel, showing the purified recombinant enzymes from *X. axonopodis* (lane 1) and *X. campestris* (lane 2). (B) Ferguson plots of molecular mass *versus* $\sqrt{K_r}$, the retardation coefficient. Molecular mass standards: ferritin (440 kDa), catalase (232 kDa), lactate dehydrogenase (140 kDa), BSA (66 kDa), carbonic anhydrase (30 kDa). Arrow indicates the $\sqrt{K_r}$ determined for both *Xanthomonas* enzymes. Inset, relative electrophoretic mobility of UDPGlcPPases from *X. axonopodis* (●) and *X. campestris* (○) as a function of polyacrylamide concentration in the gel.

Table 2
Substrate kinetic parameters of *Xca*UDPGlcPPase

Substrate	*Xca*UDPGlcPPase	
	$S_{0.5}$ (mM)	n_H
Synthesis direction		
UTP	0.21	1.0
Glc1P	0.06	1.4
Mg^{2+}	1.11	3.8
Pyrophosphorolysis direction		
UDPGlc	0.99	0.8
PPi	0.48	1.4
Mg^{2+}	0.58	1.0

shown in Fig. 3, after preincubation with UTP the enzyme exhibited a behavior that gave kinetic parameters similar to those shown in Tables 2 and 3. However, when the enzyme was preincubated with Glc1P and the reaction started with UTP the saturation pattern was different, mainly because the V_{max} was substantially decreased (Fig. 3). Similar results were observed when saturation kinetics for UTP were determined by preincubation with Glc1P or with the nucleotide.

A possible explanation for the distinct kinetic behavior could be that UDPGlcPPase undergoes a change in structure to a form with lower activity when diluted into the assay medium in the absence of UTP. Fig. 4 shows that dilution and incubation of the *Xca*UDPGlcPPase under the conditions utilized for kinetic assays, but in the absence of substrates, produced a time dependent loss of enzyme activity. The latter process was faster as the higher was the dilution of the enzyme in the incubation medium, and it became negligible at enzyme concentrations 10 μM and up (data not shown). Inactivation was modified by neither Mg^{2+}, nor by Glc1P; but UTP behaved as a very effective protector (Fig. 4). The process of enzyme inactivation followed first-order kinetics and the degree of protection afforded by UTP was dependent on the nucleotide concentration (Fig. 5). This fact was useful to calculate the dissociation constant (K_d^{UTP}) for the binding of UTP to the enzyme, utilizing the approach developed by Mildvan and Leigh [34]. In this way, K_d^{UTP} is related with the observed first-order rate constants of inactivation obtained in the absence (k') or in the presence (k'_{app}) of different concentrations of UTP by the equation:

$$\frac{1}{k'_{app}} = \frac{1}{k'} + \frac{[UTP]}{K_d^{UTP} k'} \quad (1)$$

As shown in the inset, a plot of the reciprocal k'_{app} obtained from the main Fig. 5 versus the respective UTP concentration

Table 3
Catalytic efficiency of *Xanthomonas* UDPGlcPPases for the use of UTP or TTP as a substrate

Substrate	XaxUDPGlcPPase			*Xca*UDPGlcPPase		
	k_{cat} (min^{-1})	$S_{0.5}$ (mM)	$k_{cat}/S_{0.5}$ ($min^{-1}\,mM^{-1}$)	k_{cat} (min^{-1})	$S_{0.5}$ (mM)	$k_{cat}/S_{0.5}$ ($min^{-1}\,mM^{-1}$)
UTP	1760	0.11	1.6×10^4	2400	0.21	1.1×10^4
TTP	600	0.35	1.7×10^3	406	0.36	1.1×10^3

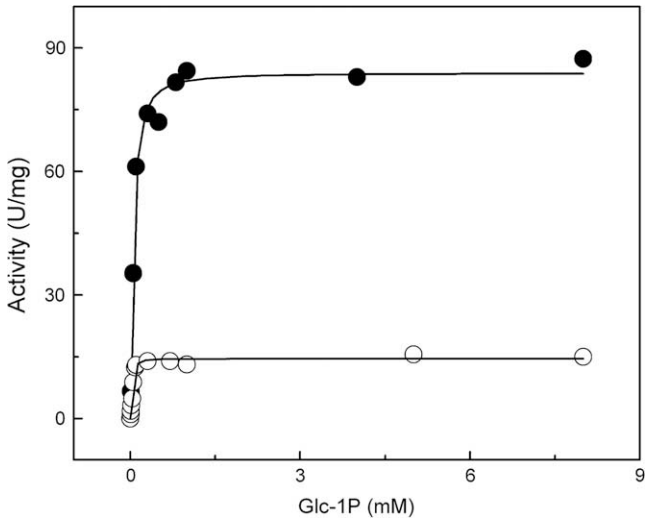

Fig. 3. Glc1P saturation curves for *Xca*UDPGlcPPase. The enzyme was preincubated in the assay medium in the presence of UTP (●), or Glc1P (○), and the reaction was initiated by the addition of the second substrate (Glc1P or UTP, respectively).

gave a straight line from which a K_d^{UTP} value of 0.015 mM was determined. This value is one order of magnitude lower than the $S_{0.5}$ calculated for the nucleotide (see Table 2), thus suggesting that the binding of UTP to the enzyme occurs with higher affinity than that estimated from kinetic measurements.

Likely, the structural variation associated with UDPGlcPPase inactivation could affect the protein oligomeric state. This was supported by results shown in Fig. 6, obtained after incubation of the enzyme under different conditions followed by crosslinking with the lysyl reagent bisuberate. Indeed, when the *Xca*UDPGlcPPase was diluted into the incubation

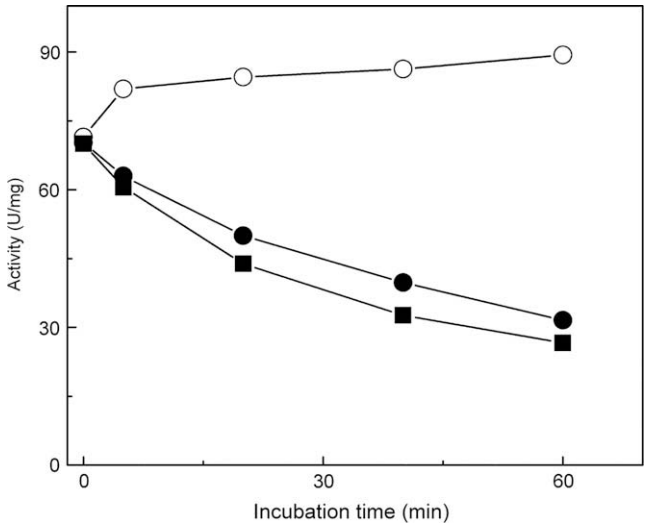

Fig. 4. Evolution of the activity of *Xca*UDPGlcPPase preincubated under different conditions. The enzyme was incubated in 80 mM MOPS, pH 8.0, in the presence of 0.2 mg/ml BSA and 7 mM $MgCl_2$ (●); plus the addition of 1.5 mM UTP (○) or 1 mM Glc1P (■). Enzyme concentration: 0.1 μM (calculated on the basis of the dimer mass).

medium without further additions, or in the presence of Glc1P or UDPGlc, low crosslinking was observed by treatment with bisuberate and a protein band of molecular mass ca. 32 kDa was predominant in SDS-PAGE (Fig. 6). The presence of UTP or TTP promoted the subunit crosslinking to form structures of higher molecular masses; being the major product thus observed a protein band of 83 kDa (2.6 times the monomer mass). The fact that the apparent size of the crosslinking product is higher than that expected for the UDPGlcPPase dimer may be attributed to the addition of mass produced by the binding of variable amounts of bisuberate (formula weight 526.4) and also to a possible impairment in SDS binding to the modified protein. Nevertheless, these results agree with the view that the nucleotide props up interaction between the enzyme subunits to form a more active oligomer.

The evolution of UDPGlcPPase activity with time after dilution, in the absence of effectors, and at different C_0 (the molar concentration of the total protein) deserved a more detailed analysis. Under the hypothesis that dissociation is responsible of enzyme inactivation, we assumed that the different inactivation curves described the evolution of the system towards the corresponding equilibrium, to reach a characteristic relationship between the dimeric and the monomeric form after dilution. Considering such an equilibrium:

$$D \underset{k_a}{\overset{k_d}{\Leftrightarrow}} 2M \tag{2}$$

the dissociation constant for the equilibrium:

$$K_D = \frac{k_d}{k_a} \tag{3}$$

can be expressed as a function of α, the degree of dissociation; and C_0, the molar concentration of the total protein assumed as a dimer, by the equation:

$$K_D = \frac{4C_0\alpha^2}{(1-\alpha)} \tag{4}$$

If equilibrium is perturbed by dilution, the velocity of dimer dissociation to a new α value can be expressed as:

$$-\frac{d}{dt}[(1-\alpha)C_0] = k_d(1-\alpha)C_0 - k_a 4\alpha^2 C_0^2 \tag{5}$$

By integrating Eq. (5) directly in its separated variables (α and t) and, after rearrangement, $(1-\alpha)$ can be expressed as a function of time (with C_0, k_d and K_D as parameters and where $\Delta = 1 + 16C_0/K_D$):

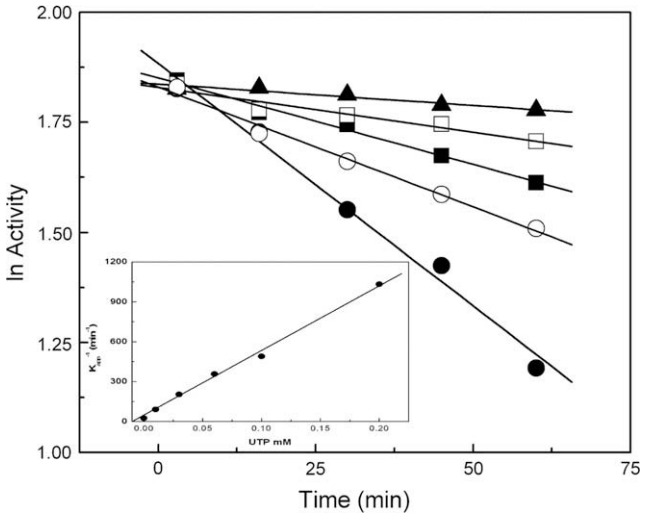

Fig. 5. Dissociation constant (K_d^{UTP}) for the interaction UDPGlcPPase-UTP calculated by the protection afforded by the substrate against inactivation of the enzyme by dilution. The enzyme (0.06 μM) was preincubated in the assay medium in the presence of different UTP concentrations: 0.01 mM (●), 0.03 mM (○), 0.06 mM (■), 0.1 mM (□) and 0.2 mM (▲). At the specified times, the enzyme reaction was initiated by the addition of Glc1P. Inset, the inverse of inactivation first-order constants (K_{app}) obtained at the different UTP concentrations were plotted as described in the text.

Fig. 7 illustrates a comparative study between experimental data, obtained from inactivation of *Xca*UDPGlcPPase (at different concentrations) after dilution into the assay medium, and theoretical curves for enzyme dissociation calculated from Eq. (6) [when integrated between limits: ($\alpha_1 = 0.01$, $t_1 = 0$) and (α, t), at the different enzyme concentrations]. As illustrated in Fig. 7, experimental points fitted fairly well with theoretical curves; after which it was possible to calculate values of K_D and k_d shown in Table 4 by resolving Eq. (6). Interestingly, at low enzyme concentrations, when the dissociation process is dominant ($\alpha \to 1$), the experimental first-order constants of inactivation were in the order of 0.04 min^{-1}, which is in good agreement with the apparent first-order dissociation constant determined at similar enzyme levels (Table 4).

As it can be observed in Table 4, K_D and k_d were not constants, as expected if true equilibrium were attained at the different enzyme concentrations. These results are better understood in the light of the model analyzed by Xu and Weber [35], where it is considered that the chemical potentials of the monomer and the dimer may vary depending on protein concentration and dissociation degree. Thus, Xu and Weber

$$1-\alpha = 1 - \left\langle \frac{\left(1-\sqrt{\Delta}\right)\cdot\left(\frac{8\cdot C_0\cdot\alpha_1+1+\sqrt{\Delta}}{8\cdot C_0\cdot\alpha_1+1-\sqrt{\Delta}}\right) - \left(1+\sqrt{\Delta}\right)\cdot e^{\left(-k_d\cdot t\cdot\sqrt{\Delta}\right)}}{\left(e^{\left(-k_d\cdot t\cdot\sqrt{\Delta}\right)} - \left(\frac{8\cdot C_0\cdot\alpha_1+1+\sqrt{\Delta}}{8\cdot C_0\cdot\alpha_1+1-\sqrt{\Delta}}\right)\right)\cdot 8\cdot\frac{C_0}{K_D}} \right\rangle \tag{6}$$

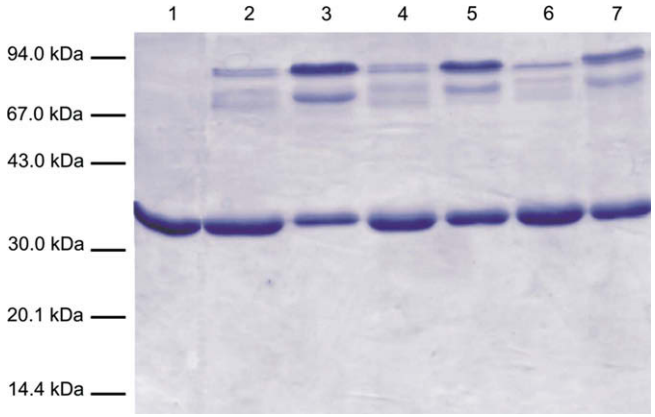

Fig. 6. SDS-PAGE of *Xca*UDPGlcPPase after crosslinking by treatment with bisuberate. The purified enzyme was incubated as specified under Section 2 in a medium containing 7 mM $MgCl_2$ in the absence (lane 1) or in the presence of 0.1 mM bisuberate alone (lane 2), or with the further addition of 1.5 mM UTP (lane 3); 1 mM Glc1P (lane 4); 1.5 mM TTP (lane 5); 1 mM UDPGlc (lane 6); or 1 mM Glc1P and 1.5 mM UTP (lane 7).

[35] performed an exhaustive analysis of oligomer association, considering the relevance of dynamics and time-averaged chemical potential of proteins. At high protein concentrations the dissociation is negligible ($\alpha \rightarrow 0$) and the chemical potentials of monomer and dimer may be considered fixed at characteristic values; but after dilution the dissociation is higher and the time spent by the protein as monomer increases (and reciprocally respect to the protein as dimer). Data in Table 4 show that K_D for the dissociation of UDPGlcPPase was variable with the different enzyme concentrations, in harmony with the view that if the monomer involved in the association equilibrium undergoes unfolding limited by its lifetime, its chemical potential will not be constant but variable, with a dependence related to the dissociation degree [35].

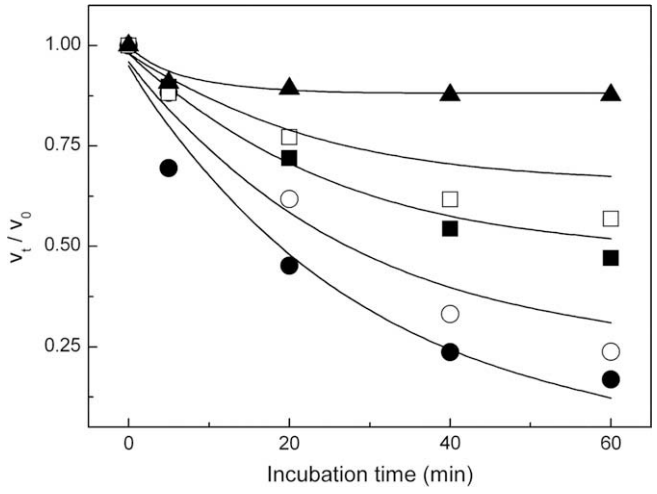

Fig. 7. Comparison between experimental inactivation data of *Xca*UDPGlcPPase and theoretical dissociation plots at different enzyme concentrations (C_0). Experimental data are represented by symbols, as relative residual activity (v_t/v_o) of the enzyme after preincubation in the assay medium. Theoretical data, represented by lines, correspond to the evolution of $(1-\alpha)$ towards equilibrium for a dimer to monomer dissociation process according to Eq. (6). Values for enzyme concentration (calculated as a dimer) were: ●, $C_0 = 0.06$ μM; ○, $C_0 = 0.5$ μM; ■, $C_0 = 1$ μM; □, $C_0 = 3$ μM; ▲, $C_0 = 5$ μM.

Table 4
Values of K_D and k_d, as defined in the text, fitting to each theoretical plot at the corresponding enzyme concentration according to Eq. (6)

Co (μM)	K_D (μM)	k_d (min^{-1})
0.06	5	0.038
0.5	4	0.029
1	2	0.015
3	2	0.014
5	0.32	0.014

The disparity in K_D values showed in Table 4 was linked to changes in G^0 (δG^0) calculated in about 1.7 kcal/mol; which correspond to a difference in the thermodynamic behavior of the dimer–monomer equilibrium at extreme dissociation conditions. The δG^0 observed for the *Xanthomonas* UDPGlcPPase is in the same order of that obtained for enolase in the earlier work reported by Xu and Weber [35], thus supposing truly minimal differences between the molecular species resultant at $\alpha = 0$ and $\alpha = 1$. As also shown in Table 4, a midpoint value for K_D is 2 μM, obtained when C_0 was 1 or 3 μM, with marked increases or decreases in K_D observed at lower or higher C_0 values, respectively. If true equilibrium is considered, each initial concentration obeys the equation $C_0 = K_D/2$ when $\alpha = 0.5$. This means that at total concentrations higher than 3 μM, or lower than 1 μM, α was, respectively, higher or lower than 0.5. The experimental equilibrium condition corresponding to $\alpha = 0.5$ was attained when $C_0 = 1$ μM and $K_D = 2$ μM. At halve dissociation, the dependence with dissociation degree is minimal and thus $K_D = 2$ μM can be considered as the more reliable thermodynamic constant for the dimer–monomer equilibrium exhibited by *Xca*UDPGlcPPase.

The molecular architecture and the active site geometry of UDPGlcPPases from, respectively, *E. coli* [7], *C. glutamicum* [36] and *S. elodea* [37] have been recently elucidated. Although these proteins were determined to be tetramers, the whole arrangement can be considered as a dimer of dimers. In fact, the dimeric nature of the *Xanthomonas* enzymes, in opposition to previously described tetramers, could be related with the very different occluded areas upon formation of the "tight" versus "loose" dimers in the 3D characterized UDPGlcPPases as tetramers (see Ref. [7,36]). On the basis of these crystallographic structures we made an in silico approach to understand, at the molecular level, the interaction between subunits that support the active dimer observed for the *Xanthomonas* enzyme. An alignment of sequences shows a good level of similarity between the enzymes from *Xanthomonas* spp. and those above indicated as solved by crystallography (see Fig. 1 of supplemental data). Specifically, degrees of identity of 37.7% and 44% were calculated for the *Xax*UDPGlcPPase with respect to the enzymes from *C. glutamicum* and *E. coli*, respectively (see Fig. 2 of supplemental data); which support the use of these proteins as templates for modeling the *Xanthomonas* enzyme. The modeled structure of *Xax*UDPGlcPPase (see Fig. 3 of supplemental data) shows two main sites for the oligomeric arrangement. One is established by the interaction between two helices at the C-terminus of

each monomer, which form the subunit–subunit interface of a tight dimeric structure, as reported from crystallography analysis [7,36]. To further evaluate this interaction, we constructed a truncated mutant enzyme, with deletion of 21 amino acid residues from the C-terminus. The shorter construct was expressed as a soluble protein that exhibited a monomeric structure and showed no catalytic activity (data not shown). These results strongly agree with the relevance of the interaction of the C-term in the association between subunits [7,36] (see also Fig. 3 of supplemental data); and also with the observation that dissociation produces a monomeric, non-active, form of the enzyme (Section 3).

The second region critical for the subunits interaction in UDPGlcPPase is that concerned with the substrate binding site (see Fig. 3 of supplemental data). As shown, the UDPGlc binding site involves the polypeptide backbone of residues Ala13, Gly14 and Gly111, and the side chains of residues Glu29, Gln106, Asp134, Glu193 and Lys194 in the *Xanthomonas* enzyme (corresponding to the conserved residues in the *C. glutamicum*). This region assembles in a three-dimensional structure exhibiting a marked proximity between two subunits (see Fig. 3 of supplemental data). As discussed from crystallographic studies [36], one main question concerning UDPGlcPPase is whether the active site is contained within one subunit or shaped by two monomers. Of interest is the contrast observed between structures of the enzyme crystals solved in the absence or in the presence of substrates [36]. This comparison shows that, although all of the residues located in the surrounding of the substrate site are contributed by one subunit, the binding of the ligand alters the structure. A main change is in the loop of an adjacent motif helix-loop-helix (Fig. 8), delineated by Tyr73 to His93 (Ser80 to Leu104 in *C. glutamicum*) that is disordered in the structure in the absence of effector and becomes ordered in its presence; after which two residues from one subunit (Arg81 and Lys84 in *Xanthomonas*; Arg89 and Lys91 in *C. glutamicum*) move closer to the active site cavity of another subunit. Thus, it is tempting to associate this latter structural analysis with the above described results concerning the higher stability of the *Xca*UDPGlcPPase in the presence of UTP. Under this view, it can be speculated that the binding of the substrate promotes small modifications in the three-dimensional structure of the active site, inducing a stronger interaction between two subunits, and stabilizing a catalytically active dimeric form of the enzyme.

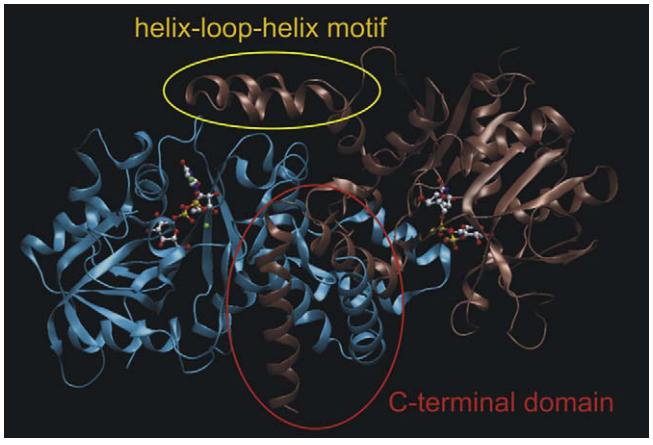

Fig. 8. Cartoon representation of the homology model of *Xax*UDPGlcPPase dimer complexed with substrate and cofactor (one UDPGlc-$(Mg^{2+})_2$ per subunit). Each subunit is represented with different colours. UDPGlc coordinated to $(Mg^{2+})_2$ is shown in a ball and stick representation. The two main regions of contact between subunits described in the text, the helix-loop-helix motif and the two C-terminal α-helices are remarked with ovals.

Interestingly, in the three-dimensional model of the *Xanthomonas* UDPGlcPPase eight different lysine residues can be identified as forming pairs between subunits in a way that they face each other being separated within 8–15 Å (Fig. 3 of supplemental data). This view agrees with the above described results on subunits crosslinking with bisuberate. This reagent has two chemical groups able to react with amino moieties of lysine residues, each group in the extreme of the bisuberate molecule that expands about 10–12 Å. As shown (Fig. 3 of supplemental data), the possible lysyl pairs close enough to crosslink two subunits after reaction with bisuberate are: Lys24-Lys36, Lys28-Lys78 or Lys28-Lys84, Lys78-Lys62, Lys84-Lys194, and Lys283-Lys283. In this way, the in silico model supports the scenario that when the enzyme adopts a dimeric structure, bisuberate could react with any of these lysyl pairs (facing contiguous and close enough) thus forming a covalent bond between the subunits.

Active forms of eukaryotic UDPGlcPPases have been reported as octamers in animals [38] and yeast [39], or monomers in protozoa [40,41] and plants [42,43]. It has been demonstrated that the plant enzyme may exist as monomer, dimer and higher order polymeric forms [42]; with oligomerization status defining the catalytic efficiency of the enzyme, which has been proposed may play a regulatory role [42–44]. These latter characteristics reported for the eukaryotic enzyme are reminiscent of results we show in the present work about substrate dependent dynamic changes in structure for the enzyme from a bacterial source. Thus, it is tempting to speculate that, even though prokaryotic and eukaryotic UDPGlcPPases are not evolutionary related [4,6,7,36], they may share some general principles of regulation via (de)polymerization or at least they may share similar binding domains.

Acknowledgments

This work was supported by grants from UNL (CAI + D 2006), CONICET (PIP No. 6358), and ANPCyT (PICT'03 01-14733, PAV'03 137, and PICTO'05 15-36129). MBB is a Postgrade Fellow from CONICET and AAI is a Principal Investigator from the same Institution.

Appendix. Supplementary figures

Supplementary figures associated with this article can be found, in the online version, at doi:10.1016/j.biochi.2008.09.001.

References

[1] S.A. Hossain, K. Tanizawa, Y. Kazuta, T. Fukui, Overproduction and characterization of recombinant UDP-glucose pyrophosphorylase from *Escherichia coli* K-12, J. Biochem. (Tokyo) 115 (1994) 965–972.

[2] P.A. Frey, The Leloir pathway: a mechanistic imperative for three enzymes to change the stereochemical configuration of a single carbon in galactose, FASEB J. 10 (1996) 461–470.

[3] H.M. Holden, I. Rayment, J.B. Thoden, Structure and function of enzymes of the Leloir pathway for galactose metabolism, J. Biol. Chem. 278 (2003) 43885–43888.

[4] M. Mollerach, R. Lopez, E. Garcia, Characterization of the galU gene of *Streptococcus pneumoniae* encoding a uridine diphosphoglucose pyrophosphorylase: a gene essential for capsular polysaccharide biosynthesis, J. Exp. Med. 188 (1998) 2047–2056.

[5] A.C. Weissborn, Q. Liu, M.K. Rumley, E.P. Kennedy, UTP: alpha-D-glucose-1-phosphate uridylyltransferase of *Escherichia coli*: isolation and DNA sequence of the galU gene and purification of the enzyme, J. Bacteriol. 176 (1994) 2611–2618.

[6] M. Mollerach, E. Garcia, The galU gene of Streptococcus pneumoniae that codes for a UDP-glucose pyrophosphorylase is highly polymorphic and suitable for molecular typing and phylogenetic studies, Gene 260 (2000) 77–86.

[7] J.B. Thoden, H.M. Holden, The molecular architecture of glucose-1-phosphate uridylyltransferase, Protein Sci. 16 (2007) 432–440.

[8] L. Bonofiglio, E. Garcia, M. Mollerach, Biochemical characterization of the pneumococcal glucose 1-phosphate uridylyltransferase (GalU) essential for capsule biosynthesis, Curr. Microbiol. 51 (2005) 217–221.

[9] H.Y. Chang, J.H. Lee, W.L. Deng, T.F. Fu, H.L. Peng, Virulence and outer membrane properties of a galU mutant of Klebsiella pneumoniae CG43, Microb. Pathog. 20 (1996) 255–261.

[10] C.R. Dean, J.B. Goldberg, Pseudomonas aeruginosa galU is required for a complete lipopolysaccharide core and repairs a secondary mutation in a PA103 (serogroup O11) wbpM mutant, FEMS Microbiol. Lett. 210 (2002) 277–283.

[11] R.C. Sandlin, K.A. Lampel, S.P. Keasler, M.B. Goldberg, A.L. Stolzer, A.T. Maurelli, A virulence of rough mutants of *Shigella flexneri*: requirement of O antigen for correct unipolar localization of IcsA in the bacterial outer membrane, Infect. Immun. 63 (1995) 229–237.

[12] C. Wandersman, S. Letoffe, Involvement of lipopolysaccharide in the secretion of Escherichia coli alpha-haemolysin and *Erwinia chrysanthemi* proteases, Mol. Microbiol. 7 (1993) 141–150.

[13] E. Silva, A.R. Marques, A.M. Fialho, A.T. Granja, I. Sa-Correia, Proteins encoded by *Sphingomonas elodea* ATCC 31461 rmlA and ugpG genes, involved in gellan gum biosynthesis, exhibit both dTDP- and UDP-glucose pyrophosphorylase activities, Appl. Environ. Microbiol. 71 (2005) 4703–4712.

[14] A. Becker, F. Katzen, A. Puhler, L. Ielpi, Xanthan gum biosynthesis and application: a biochemical/genetic perspective, Appl. Microbiol. Biotechnol. 50 (1998) 145–152.

[15] G. Dunger, V.M. Relling, M.L. Tondo, M. Barreras, L. Ielpi, E.G. Orellano, J. Ottado, Xanthan is not essential for pathogenicity in citrus canker but contributes to *Xanthomonas* epiphytic survival, Arch. Microbiol. 188 (2007) 127–135.

[16] A.A. Vojnov, H. Slater, M.J. Daniels, J.M. Dow, Expression of the gum operon directing xanthan biosynthesis in *Xanthomonas campestris* and its regulation in planta, Mol. Plant. Microbe Interact. 14 (2001) 768–774.

[17] L.A. Rigano, F. Siciliano, R. Enrique, L. Sendin, P. Filippone, P.S. Torres, J. Questa, J.M. Dow, A.P. Castagnaro, A.A. Vojnov, M.R. Marano, Biofilm formation, epiphytic fitness, and canker development in *Xanthomonas axonopodis* pv. *citri*, Mol. Plant Microbe Interact. 20 (2007) 1222–1230.

[18] C.L. Wei, N.T. Lin, S.F. Weng, Y.H. Tseng, The gene encoding UDP-glucose pyrophosphorylase is required for the synthesis of xanthan gum in *Xanthomonas campestris*, Biochem. Biophys. Res. Commun. 226 (1996) 607–612.

[19] M.P. Marzocca, N.E. Harding, E.A. Petroni, J.M. Cleary, L. Ielpi, Location and cloning of the ketal pyruvate transferase gene of *Xanthomonas campestris*, J. Bacteriol. 173 (1991) 7519–7524.

[20] T.F. Maniatis, E.F. Fritsch, J. Sambrook, Molecular Cloning: A Laboratory Manual, Cold Spring Harbor Laboratory, New York, 1982.

[21] C. Fusari, A.M. Demonte, C.M. Figueroa, M. Aleanzi, A.A. Iglesias, A colorimetric method for the assay of ADP-glucose pyrophosphorylase, Anal. Biochem. 352 (2006) 145–147.

[22] M.K. Morell, M. Bloom, V. Knowles, J. Preiss, Subunit structure of spinach leaf ADPglucose pyrophosphorylase, Plant Physiol. 85 (1987) 182–187.

[23] M.M. Bradford, A rapid and sensitive method for the quantitation of microgram quantities of protein utilizing the principle of protein–dye binding, Anal. Biochem. 72 (1976) 248–254.

[24] U.K. Laemmli, Cleavage of structural proteins during the assembly of the head of bacteriophage T4, Nature 227 (1970) 680–685.

[25] K.A. Ferguson, Starch-gel electrophoresis – application to the classification of pituitary proteins and polypeptides, Metabolism 13 (1964) 985–1002.

[26] J.V. Staros, *N*-hydroxysulfosuccinimide active esters: bis(*N*-hydroxysulfosuccinimide) esters of two dicarboxylic acids are hydrophilic, membrane-impermeant, protein cross-linkers, Biochemistry 21 (1982) 3950–3955.

[27] A. Sali, T.L. Blundell, Comparative protein modelling by satisfaction of spatial restraints, J. Mol. Biol. 234 (1993) 779–815.

[28] A. Fiser, R.K. Do, A. Sali, Modeling of loops in protein structures, Protein Sci. 9 (2000) 1753–1773.

[29] M.A. Marti-Renom, A.C. Stuart, A. Fiser, R. Sanchez, F. Melo, A. Sali, Comparative protein structure modeling of genes and genomes, Annu. Rev. Biophys. Biomol. Struct. 29 (2000) 291–325.

[30] R. Sanchez, A. Sali, Comparative protein structure modeling. Introduction and practical examples with modeller, Methods Mol. Biol. 143 (2000) 97–129.

[31] N. Eswar, B. John, N. Mirkovic, A. Fiser, V.A. Ilyin, U. Pieper, A.C. Stuart, M.A. Marti-Renom, M.S. Madhusudhan, B. Yerkovich, A. Sali, Tools for comparative protein structure modeling and analysis, Nucleic Acids Res. 31 (2003) 3375–3380.

[32] D. Rodbard, A. Chrambach, Unified theory for gel electrophoresis and gel filtration, Proc Natl Acad Sci USA 65 (1970) 970–977.

[33] A. Chrambach, D. Rodbard, Polyacrylamide gel electrophoresis, Science 172 (1971) 440–451.

[34] A.S. Mildvan, R.A. Leigh, Deternation of co-factor dissociation constants from the kinetics of inhibition of enzymes, Biochim. Biophys. Acta 89 (1964) 393–397.

[35] G. Xu, G. Weber, Dynamics and time-averaged chemical potential of proteins: importance in oligomer association, Proc Natl Acad Sci USA 79 (1982) 5268–5271.

[36] J.B. Thoden, H.M. Holden, Active site geometry of glucose-1-phosphate uridylyltransferase, Protein Sci. 16 (2007) 1379–1388.

[37] D. Aragao, A.M. Fialho, A.R. Marques, E.P. Mitchell, I. Sa-Correia, C. Frazao, The complex of *Sphingomonas elodea* ATCC 31461 glucose-1-phosphate uridylyltransferase with glucose-1-phosphate reveals a novel quaternary structure, unique among nucleoside diphosphate--sugar pyrophosphorylase members, J. Bacteriol. 189 (2007) 4520–4528.

[38] R.L. Turnquist, R.G. Hansen, Uridine Diphosphoryl Glucose Pyrophosphorylase, vol. 8A, Academic Press, New York and London, 1973, 51–71.

[39] A. Roeben, J.M. Plitzko, R. Korner, U.M. Bottcher, K. Siegers, M. Hayer-Hartl, A. Bracher, Structural basis for subunit assembly in UDP-glucose pyrophosphorylase from *Saccharomyces cerevisiae*, J. Mol. Biol. 364 (2006) 551–560.

[40] A.C. Lamerz, T. Haselhorst, A.K. Bergfeld, M. von Itzstein, R. Gerardy-Schahn, Molecular cloning of the Leishmania major UDP-glucose pyrophosphorylase, functional characterization, and ligand binding analyses using NMR spectroscopy, J. Biol. Chem. 281 (2006) 16,314–16,322.

[41] T. Steiner, A.C. Lamerz, P. Hess, C. Breithaupt, S. Krapp, G. Bourenkov, R. Huber, R. Gerardy-Schahn, U. Jacob, Open and closed structures of the UDP-glucose pyrophosphorylase from Leishmania major, J. Biol. Chem. 282 (2007) 13,003–13,010.

[42] F. Martz, M. Wilczynska, L.A. Kleczkowski, Oligomerization status, with the monomer as active species, defines catalytic efficiency of UDP-glucose pyrophosphorylase, Biochem. J. 367 (2002) 295–300.

[43] J.G. McCoy, E. Bitto, C.A. Bingman, G.E. Wesenberg, R.M. Bannen, D.A. Kondrashov, G.N. Phillips Jr., Structure and dynamics of UDP-glucose pyrophosphorylase from *Arabidopsis thaliana* with bound UDP-glucose and UTP, J. Mol. Biol. 366 (2007) 830–841.

[44] L.A. Kleczkowski, F. Martz, M. Wilczynska, Factors affecting oligomerization status of UDP-glucose pyrophosphorylase, Phytochemistry 66 (2005) 2815–2821.